PROJECT REPORT

HØGSKOLEN I ÅLESUND

Aalesund University College

TITLE:
Multi-body dynamics modelling using Bond Graph method

CANDIDATE(S):
2304

DATE:	COURSE CODE:	COURSE TITLE:	RESTRICTION:
09.12.2014	IP504813	Modelling and Simulation of Dynamic Systems	

STUDY PROGRAME:	PAGES/APPENDIX:	LIBRARY NO.:
Product and System Design	19/0	

SUPERVISOR(S):
Vilmar Æsøy, Houxiang Zhang

SUMMARY:

This document is an internal evaluation report for a master course in Product and System Design at Aalesund University College.

The course is designed to study the principles of modelling and simulation of dynamic systems in engineering fields, and to understand the process of modelling from basic physical laws to mathematical models. Different methods and tools are involved in the course to perform dynamic simulation of multi-disciplinary systems. Specifically, Bond Graph (BG) method is introduced as well as a simulation software tool based on BG 20sim. The knowledge in BG basics is important for the following study of the master program. More complex systems will be studied and BG method will be introduced in deeper levels as a general approach for modelling of multi-disciplinary systems.

The project work in this report presents the modelling process of multi-body dynamics using BG method. Multi-body mechanisms are found in various engineering industries, for example, robotic manipulators, and cranes. In particular, to study the dynamics of maritime cranes is of significant interest in offshore and subsea operations due the fact of heave lifting and unstable working platform. As case study, a common type of maritime crane with three degree of freedoms operating in three dimensions is implemented.

This report is submitted by students for evaluation at Ålesund University College.

Postal adress:	Visit adress	Telephone	Fax	Bank
Høgskolen i Ålesund	Larsgårdsvegen 2	70 16 12 00	70 16 13 00	7694 05 00636
N-6025 Ålesund	**Internett**	**E-mail**		**Enterprise no.**
Norway	www.hials.no	postmottak@hials.no		NO 971 572 140

TABLE OF CONTENTS

SUMMARY

This document is an internal evaluation report for a master course in Product and System Design at Aalesund University College.

The course is designed to study the principles of modelling and simulation of dynamic systems in engineering fields, and to understand the process of modelling from basic physical laws to mathematical models. Different methods and tools are involved in the course to perform dynamic simulation of multi-disciplinary systems. Specifically, Bond Graph (BG) method is introduced as well as a simulation software tool based on BG 20sim. The knowledge in BG basics is important for the following study of the master program. More complex systems will be studied and BG method will be introduced in deeper levels as a general approach for modelling of multi-disciplinary systems.

The project work in this report presents the modelling process of multi-body dynamics using BG method. Multi-body mechanisms are found in various engineering industries, for example, robotic manipulators, and cranes. In particular, to study the dynamics of maritime cranes is of significant interest in offshore and subsea operations due the fact of heave lifting and unstable working platform. As case study, a common type of maritime crane with three degree of freedoms operating in three dimensions is implemented.

1 INTRODUCTION

In recent years, more and more interest is raised in modelling and simulation of multi-disciplinary dynamic systems, in form of either mathematic model or actual hardware. The physical worlds of various disciplinary are so different that different physical laws applied in describing their dynamics. Modelling and simulation of these systems each has its own methodology and software preference. These approaches and tools have proved of great value and benefits to be used. To reuse the existing knowledge, one of the major challenges is the interfacing and interaction between the sub-models.

Maritime cranes are found on-board almost all kinds of vessels and platforms for handling personnel and cargo, lifting heave objects, towing and recovering operations and so on. Cranes on-board vessels and platforms handling goods between the quayside and vessel or between vessels are normally referred to as offshore cranes. Cranes that are used for handling submerged loads as well e.g. launch and recovery of submersibles or installation of subsea hardware, are normally referred to as subsea cranes. Compare to land based cranes with a solid fixed base, offshore and subsea cranes are subject to significant dynamic forces from the resulting payload sway directly or indirectly caused by the vessel motion. As field testing in maritime industry is rather expensive and time consuming to carry out and subject to many factors such as weather condition and vessel availability, modelling and simulation become a crucial part for product design, testing and analysis.

In previous literature, several modelling approaches and software tools can be identified for multi-body dynamics modelling and simulation. Bond Graph method is a modelling technique by describing the energy structure of the physical system. Based on the energy conservation law, models that involve different energy domains can be developed using the same generalized variables, namely effort and flow, of which the product is power. The software tool for modelling and simulation is called 20-sim. A 3D animation scene is created for the visualization of the operation.

This report work presents a Bond Graph (BG) model of a common type of maritime crane (Figure 1) composed of three revolute joints operating in three dimensions. The multi-body dynamic model takes care of the mechanical properties of the system and simulation of operational behaviors. The model provides interfaces to models of control system, actuators and sensors, which is important for simulation of maritime crane and winch operations. Maritime operations are challenging due to its inherited nature in heavy lifting, system stiffness and load sway impacted by the unstable working platform. Modelling and simulation of offshore operations in virtual environment is becoming an increasingly demanded yet beneficial process during product and system design, new component and control algorithm testing, as well as operator training. The model is a building block for simulation of the control of the lifting operations.

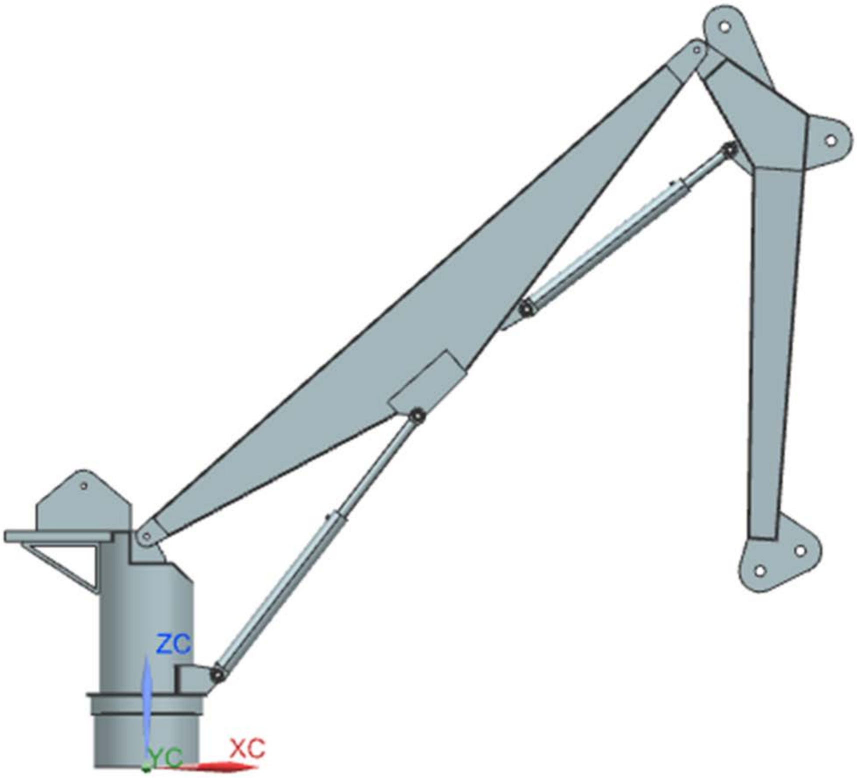

Figure 1. A knuckle boom crane

2 MULTI-BODY DYNAMICS

Multi-body mechanisms, like robotic manipulators and cranes, are driven by electric, hydraulic or pneumatic actuators, which provide forces or torques to the joints of the mechanisms. Maritime cranes are generally much larger in size and heavier in lifting capacity compare to robotic manipulators, while they are slower in motions and with fewer degrees of freedoms. To ensure the stability of operation, maritime cranes are usually hydraulic actuated. The dynamics describes how the mechanism behaves in response to the actuator forces or torques. For simplicity, the dynamics of the actuators themselves are not considered, and hence arbitrary forces and torques are applied to the joints.

2.1 Lagrange's Equations

Many approaches exist for deriving the dynamic equations of a mechanical system. All methods generates equivalent sets of equations, however different forms of these equations are better suit for computation and analysis of different purposes. Lagrange's approach is introduced here for our derivation which relies on the energy properties of the mechanism to compute the equations of motion. These equations are particularly useful for modelling using Bond Graph, and by this algebraic loops and derivative causality problems are avoided when modelling non-liner mechanical systems. Implementation of Bond Graph will be discussed more in later chapters.

The equations of motion for a mechanical system with generalized coordinates q are given by

$$\frac{d}{dt}\frac{\partial L}{\partial \dot{q}_i} - \frac{\partial L}{\partial q_i} = E_i$$

Where $L(q,\dot{q}) = T(q,\dot{q}) - V(q)$ is the difference between the kinetic energy and potential energy of the system. E_i is the external force or torque acting on the ith generalized coordinate.

Lagrange's equations are an elegant formulation of the dynamics of a mechanical system as it reduces the equations needed to describe the motion of the system using generalized coordinates instead of all the bodies with mass and inertia properties.

2.2 Example: Dynamics of a 1-DOF revolute pendulum link

An ideal rigid link with one end attached to a revolute joint is shown in Figure 2. The centre of mass is localised in the middle of the link with mass m. The revolute joint (z-axis) gives one degree of freedom to the link denoted by angle *Ɵ.* We now solve the motion of the link under the impact of the gravity force.

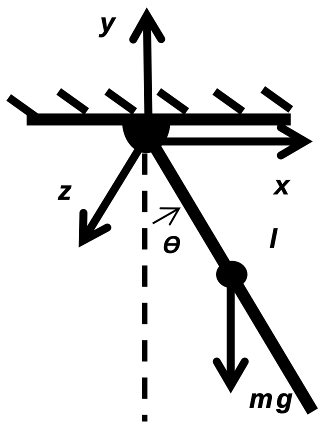

Figure 2 Ideal 1-DOF revolute pendulum link

The generalized coordinates is the angle *Ɵ,* from which the positions of the link, x, y, z can be determined.

The kinetic energy of the link is:

$$T = \frac{1}{2}mv^2 + \frac{1}{2}I\dot{\theta}^2 = \frac{1}{6}ml^2\dot{\theta}^2$$

Where $v = \frac{1}{2}l\dot{\theta}, I = \frac{1}{12}ml^2$

The potential energy of the link is:

$$V = -\frac{1}{2}mglcos\theta$$

The Lagrange's equations give:

$$\frac{d}{dt}\left(\frac{\partial L}{\partial \dot{\theta}}\right) = \frac{1}{3}ml^2\ddot{\theta}$$

$$\frac{\partial L}{\partial \theta} = \frac{1}{2}mglsin\theta$$

And finally the dynamics satisfy:

$$\frac{1}{3}ml^2\ddot{\theta} - \frac{1}{2}mglsin\theta = 0$$

To apply the Lagrange's equations to a multi-link mechanism, like a robotic arm or a crane, we must write the kinetic energy and potential energy as functions of the joint angles and velocities, i.e. using the joint angles and velocities as generalized coordinates. Since each link is assumed as a rigid body, its kinematic and potential energy can be defined in terms of mass and momentum of inertia about the centre of mass.

2.3 Example: Dynamics of a 2-DOF revolute planar robot

To illustrate how Lagrange's equations apply to multi-link mechanisms, a simple two-link robotic arm with two revolute joints moving in a planar is shown, Figure 3.

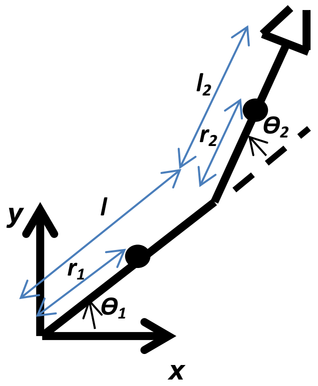

Figure 3 Two-link planar robotic arm

The kinetic energy is given:

$$T(\theta_1, \dot{\theta}_1, \theta_2, \dot{\theta}_2) = \frac{1}{2} m_1 v_1{}^2 + \frac{1}{2} I_1 \dot{\theta}_1{}^2 + \frac{1}{2} m_2 v_2{}^2 + \frac{1}{2} I_2 \dot{\theta}_2{}^2$$

The velocity of the centre of mass v is the magnitude of the velocity in x, y axis.

$$x_1 = r_1 c_1$$

$$y_1 = r_1 s_1$$

$$\dot{x_1} = -r_1 s_1 \dot{\theta}_1$$

$$\dot{y_1} = r_1 c_1 \dot{\theta}_1$$

$$x_2 = l_1 c_1 + r_2 c_{12}$$

$$y_2 = l_1 s_1 + r_2 s_{12}$$

$$\dot{x_2} = -(l_1 s_1 + r_2 s_{12}) \dot{\theta}_1 - r_2 s_{12} \dot{\theta}_2$$

$$\dot{y_2} == (l_1 c_1 + r_2 c_{12}) \dot{\theta}_1 + r_2 c_{12} \dot{\theta}_2$$

The potential energy is given by:

$$V(\theta_1, \theta_2) = m_1 g r_1 s_1 + m_2 g (l_1 s_1 + r_2 s_{12})$$

Substitute the above equations and after some manipulation:

The Lagrange's equations give:

$$\frac{d}{dt} \frac{\partial L}{\partial \dot{\theta}} = \begin{bmatrix} m_1 r_1{}^2 + I_1 + m_2 \left(l_1{}^2 + r_1{}^2 + 2 l_1 r_2 c_2\right) + I_2 & m_2 (l_1 r_2 c_2 + r_2{}^2) + I_2 \\ m_2 (l_1 r_2 c_2 + r_2{}^2) + I_2 & m_2 r_2{}^2 + I_2 \end{bmatrix} \begin{bmatrix} \ddot{\theta}_1 \\ \ddot{\theta}_2 \end{bmatrix}$$

$$\frac{\partial L}{\partial \theta} = \begin{bmatrix} -m_2 l_1 r_2 s_2 \dot{\theta}_2 - m_1 g r_1 c_1 - m_2 g (l_1 c_1 + r_2 c_{12}) & m_2 l_1 r_2 s_2 \dot{\theta}_1 \\ -m_2 l_1 r_2 s_2 \left(\dot{\theta}_1 + \dot{\theta}_2\right) & -m_2 g r_2 c_{12} \end{bmatrix} \begin{bmatrix} \dot{\theta}_1 \\ \dot{\theta}_2 \end{bmatrix}$$

And finally the dynamics satisfy:

$$\begin{bmatrix} m_1 r_1{}^2 + I_1 + m_2 \left(l_1{}^2 + r_1{}^2 + 2 l_1 r_2 c_2\right) + I_2 & m_2 (l_1 r_2 c_2 + r_2{}^2) + I_2 \\ m_2 (l_1 r_2 c_2 + r_2{}^2) + I_2 & m_2 r_2{}^2 + I_2 \end{bmatrix} \begin{bmatrix} \ddot{\theta}_1 \\ \ddot{\theta}_2 \end{bmatrix} + \begin{bmatrix} -m_2 l_1 r_2 s_2 \dot{\theta}_2 - m_1 g r_1 c_1 - m_2 g (l_1 c_1 + r_2 c_{12}) & m_2 l_1 r_2 s_2 \dot{\theta}_1 \\ -m_2 l_1 r_2 s_2 \left(\dot{\theta}_1 + \dot{\theta}_2\right) & -m_2 g r_2 c_{12} \end{bmatrix} \begin{bmatrix} \dot{\theta}_1 \\ \dot{\theta}_2 \end{bmatrix} = \begin{bmatrix} E_1 \\ E_2 \end{bmatrix}$$

3 BOND GRAPH REPRESENTATION

Classic Newton-Euler method for deriving dynamic equations is not introduced here. Representation using bond graph is straight forward and gives explicit differential equations, Figure 4. The general coordinates are then the velocities of the centre of mass and the angle. The constrain is defined by the displacements in x, y axis at the joint, simply described by a spring-damper. The relationships between the general coordinates and the constrain as well as external forces including the gravity are represented by MTF-element in Bong Graph.

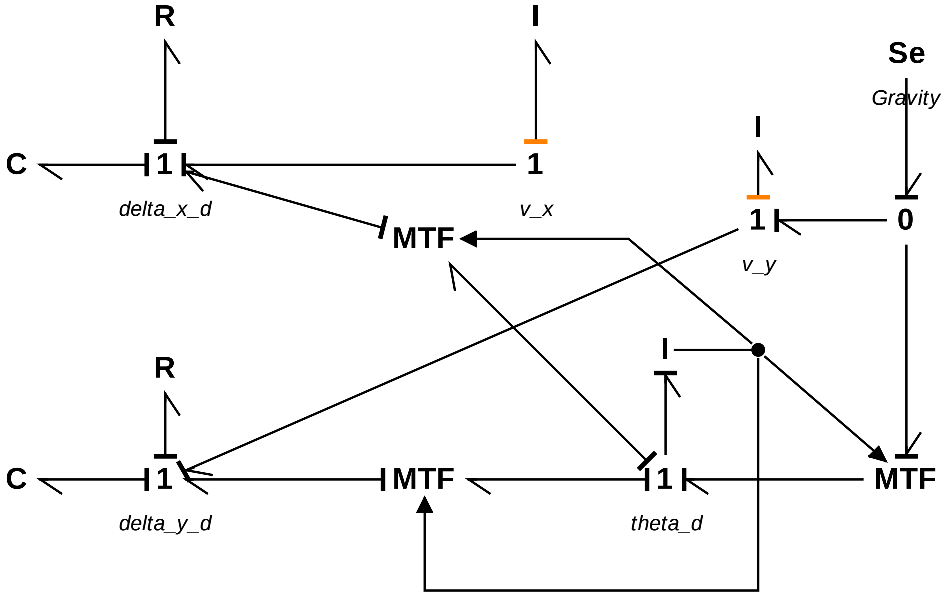

Figure 4. Bond Graph representation of 1-DOF revolute pendulum link

3.1 IC-field

A special type of IC-field is introduced here, the equations of which are the Lagrange's equations in a Hamiltonian form. The generalized coordinates are the joint angles and joint velocities. Define generalized momenta p_i and generalised forces e_i' in terms of the displacement q_i by:

$$p_i = \frac{\partial L}{\partial \dot{q}_\iota}$$

$$e_i' = \frac{\partial L}{\partial \dot{q}_\iota}$$

The Lagrange's equations can be rewritten in momentum form (Hamiltonian form):

$$\dot{p}_\iota = e_i' + E_i$$

The IC-field representation of the Hamiltonian form of Lagrange's equations can be established, Figure 5:

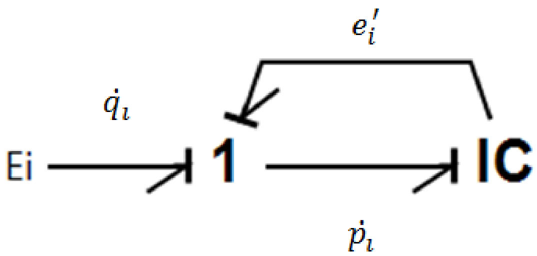

Figure 5. IC-field representation of the Hamiltonian form of Lagrange's equations

3.2 Implementation of the 1-DOF revolute pendulum link using IC-field

The equations inside the IC-field may appear complex, but it use less generalised coordinates to represent a multi-body system in a more clean form. Figure 6 shows the model of the 1-DOF revolute pendulum link using IC-field. And Figure 7 are the plotting results of the joint angle (a) under impact of the gravity, the end tip position (b) and 3D animation (b).

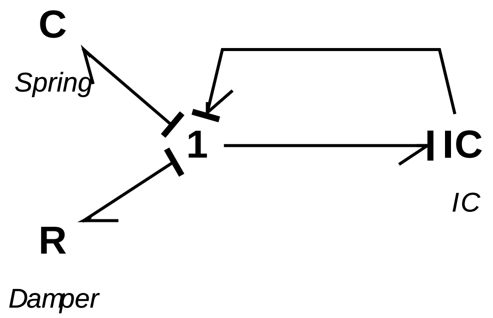

Figure 6. IC-field representation of the 1-DOF revolute pendulum link

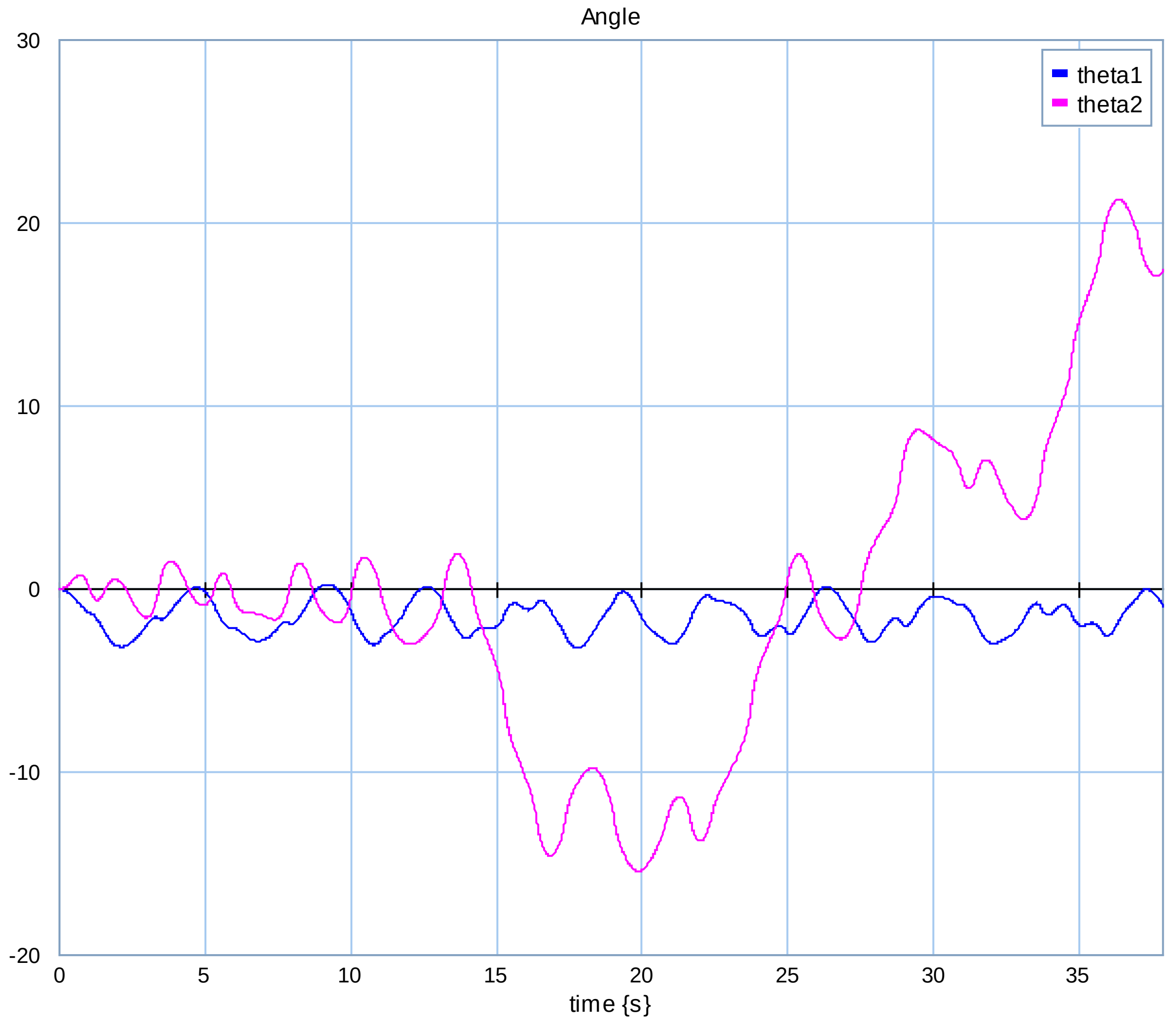

(a)

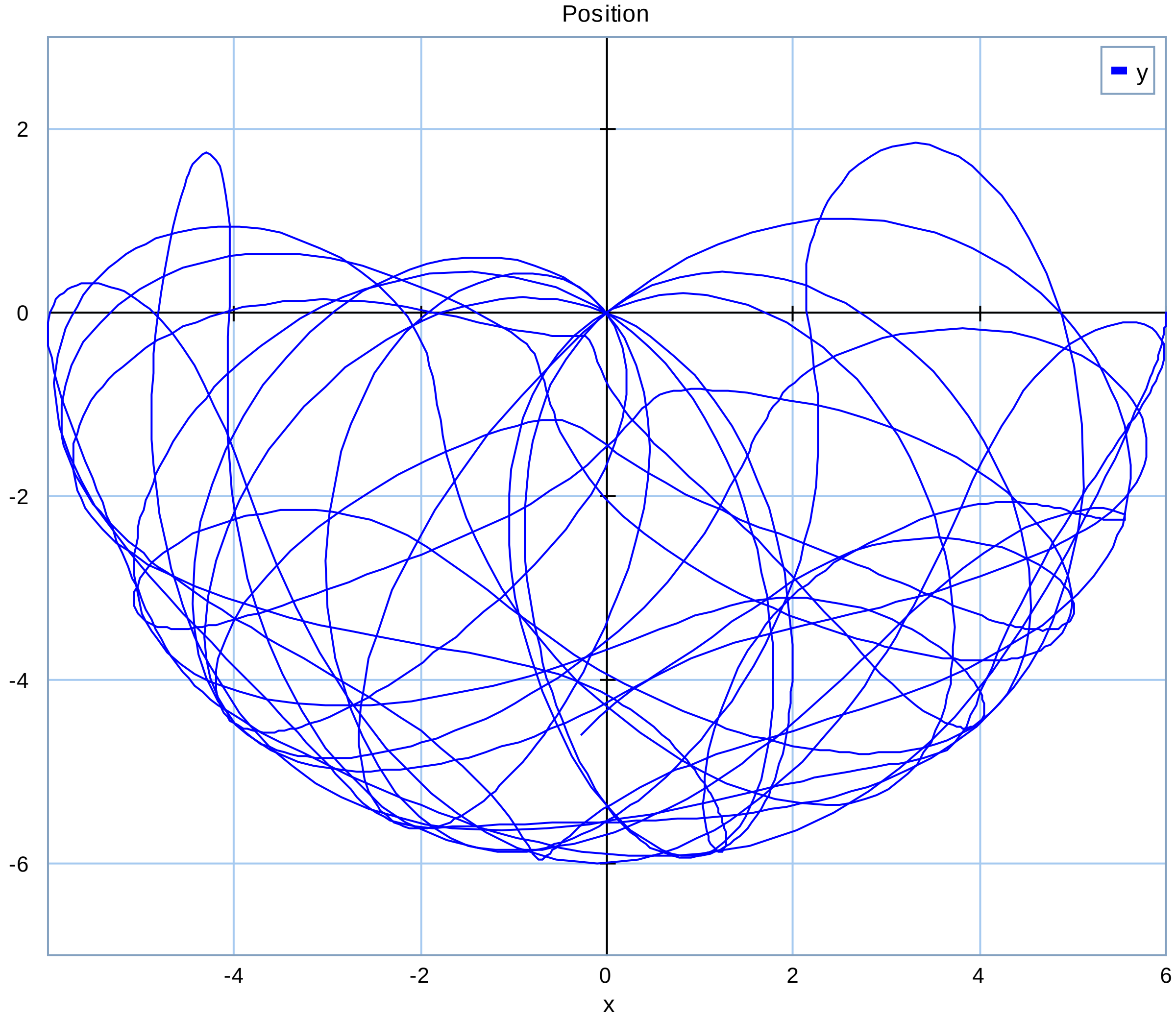

(b)

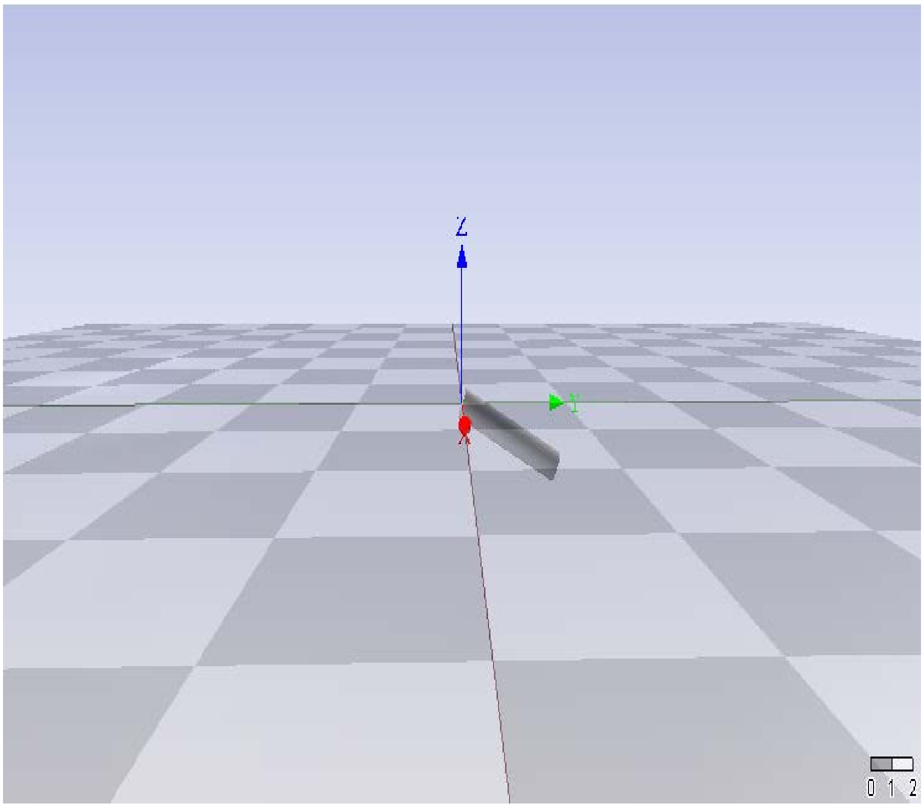

(c)

Figure 7. (a) Joint angle with/without joint friction (b) the trajectory of the end tip position (c) 3D animation

To extend the pendulum model by adding actuation torques to the joint or forces to the link gives us a simple crane model, Figure 8. The control signal uses a keyboard for the cylinder force. Plotting results of the joint angles and 3D animation scene is presented, Figure 9.

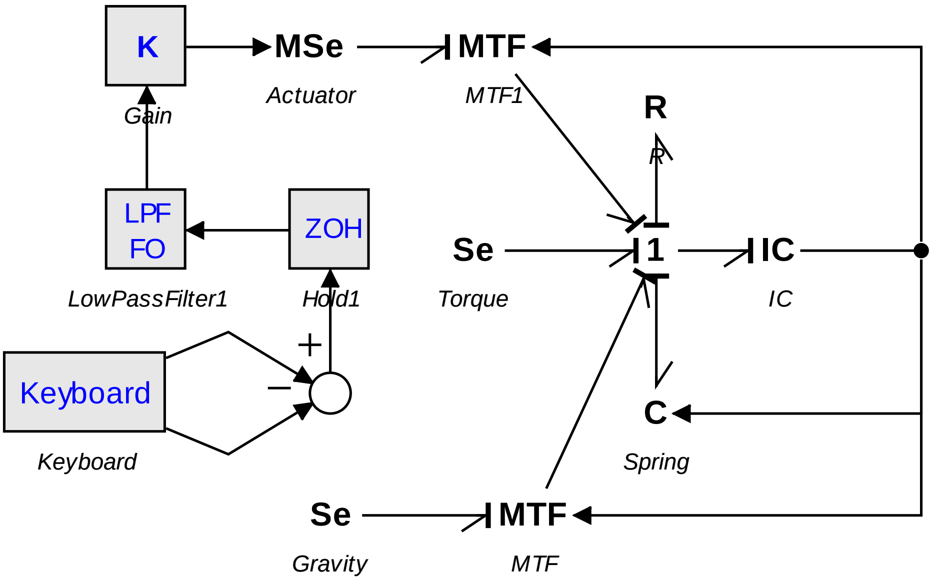

Figure 8. 1-DOF simple crane with actuators

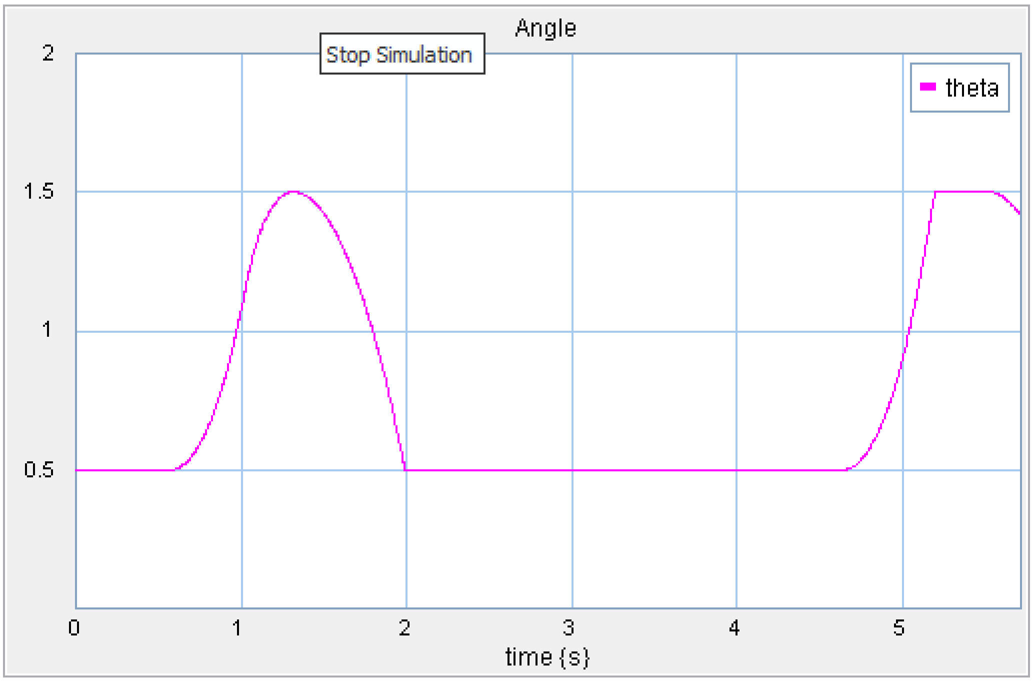

(a) Joint angle in radians

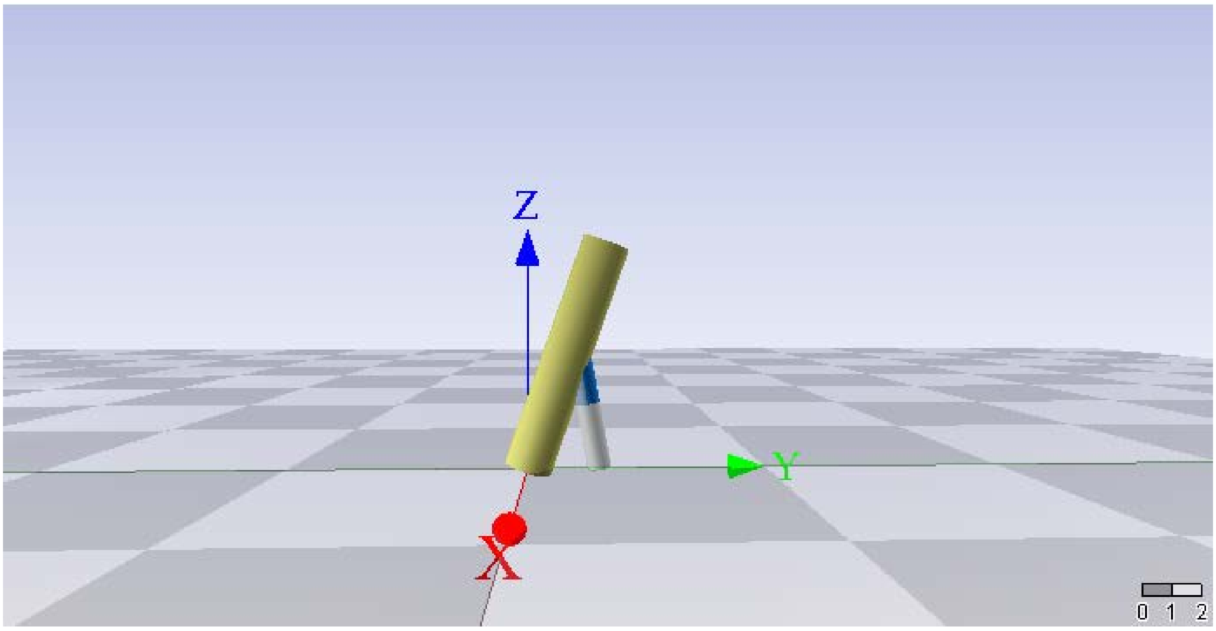

(b) 3D animation using simple blocks

Figure 9. Plotting of the joint and angle and 3D animation scene

3.3 Implementation of the 2-DOF revolute robotic arm using IC field

Furthermore, when many inertial elements are highly constrained, only a few degrees of freedom, i.e. generalised coordinates, are necessary to describe the motion of the system. Derivative causality will appear when these elements are connected. For example, Figure 10 shows the representation of the 2-DOF revolute robotic arm using normal bond graphs. The model cannot be solved explicitly as derivative causality exists.

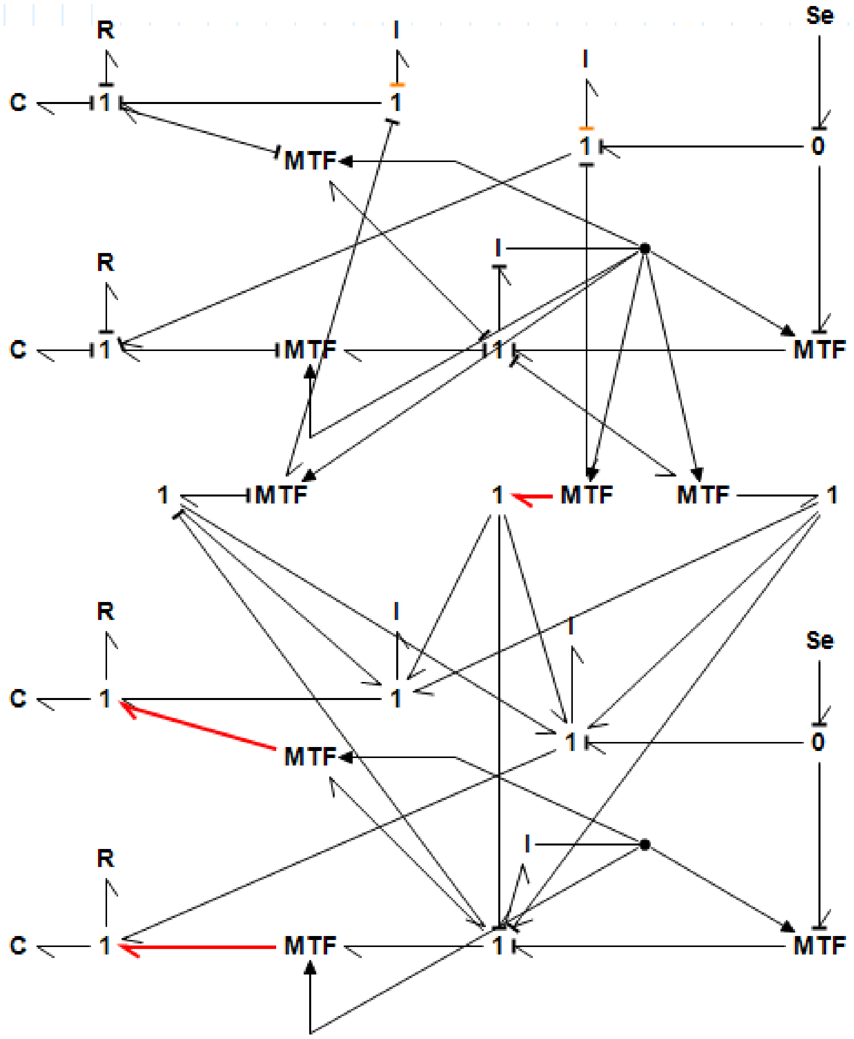

Figure 10. Bond Graph representation of the 2-DOF revolute robotic arm

Using IC-field the 2-DOF revolute robotic arm model is shown, Figure 11. External torques and forces can be added fairly easily as well. A plotting result of the joints angles and 3D animation scene are presented of the damped 2-DOF robotic arm under the impact of gravity, Figure 12.

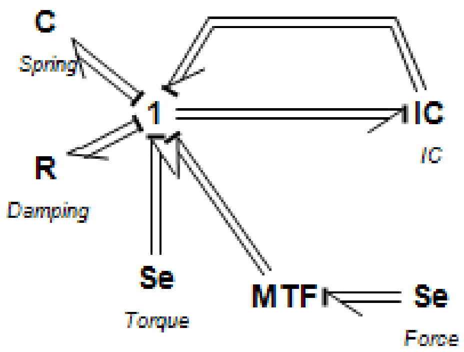

Figure 11. IC-field representation of the 2-DOF revolute robotic arm

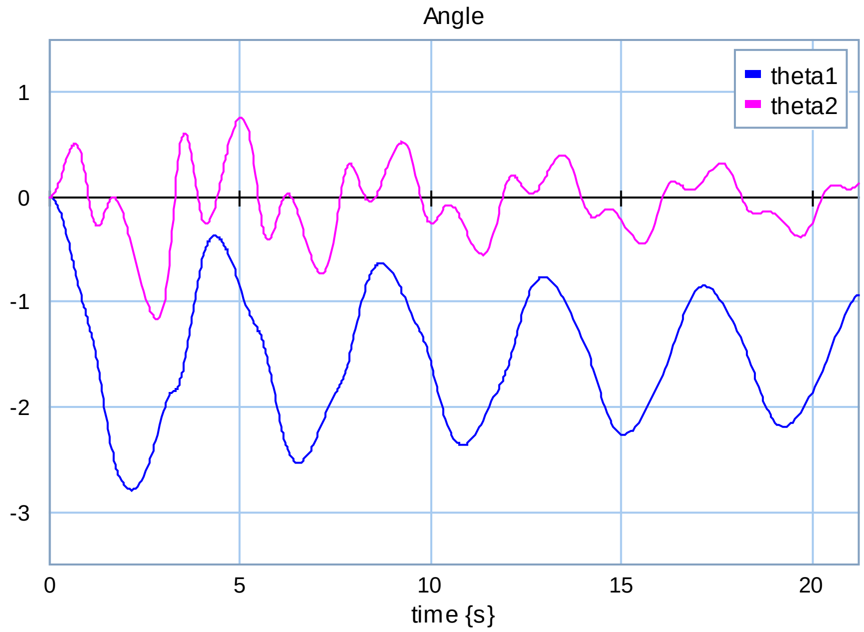

(a)

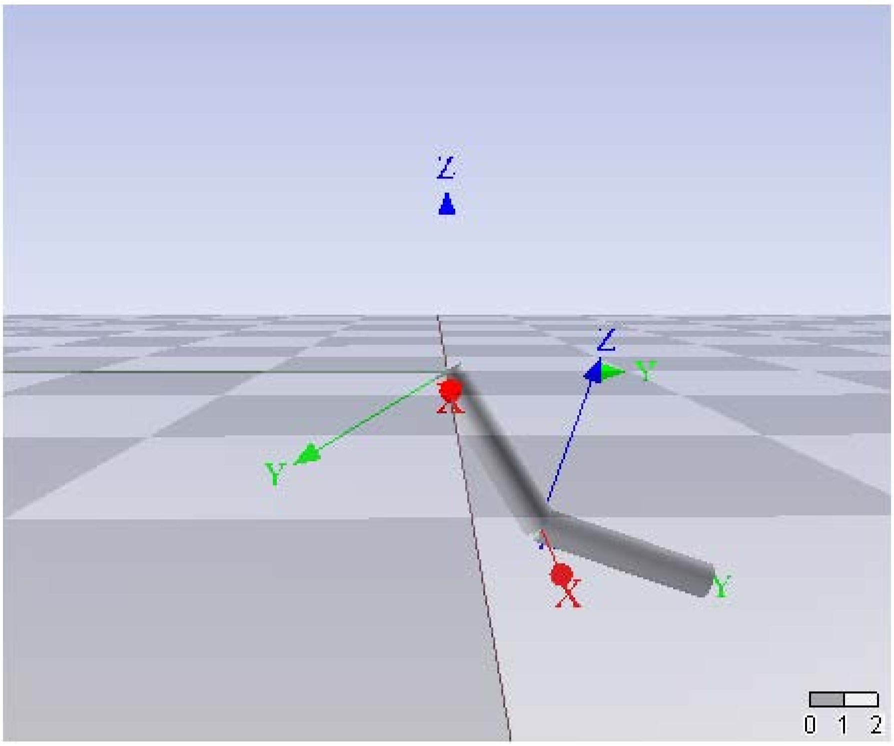

(b)

Figure 12. Plotting of the joints angles (a) and 3D animation scene (b)

4 DYNAMICS OF THE 3-DOF REVOLUTE MARITIME CRANE AND BOND GRAPH REPRESENTATION USING IC-FIELD

To calculate the kinetic and potential energy of the crane with 3 joints and 3 links, we define a coordinate frame attached to the centre of mass of each link. The velocity of the centre of mass of the ith link is given by:

$$v_i = J_i(\theta)\dot{\theta}$$

Where $J_i(\theta)$ is the Jacobian from the ith link to the base frame.

The kinetic energy is:

$$T_i(\theta,\dot{\theta}) = \frac{1}{2}v_i^T M_i v_i = \frac{1}{2}\theta_i^T J_i^T(\theta) M_i J_i(\theta)\dot{\theta}$$

Where M_i is the generalised inertia matrix for the ith link. If the assigned local frame is aligned with the inertia axis of the link, the inertia matrix M_i has the following general form:

$$M_i = \begin{bmatrix} m_i & & & & & \\ & m_i & & & & \\ & & m_i & & & \\ & & & I_{xi} & & \\ & & & & I_{yi} & \\ & & & & & I_{zi} \end{bmatrix}$$

The total kinetic energy can be written:

$$T(\theta,\dot{\theta}) = \sum_{i=1}^{n} T_i(\theta,\dot{\theta}) = \frac{1}{2}\dot{\theta}^T M(\theta)\dot{\theta}$$

Here define $M(\theta)$ is the inertia matrix of the crane

$$M(\theta) = \sum_{i=1}^{n} J_i^T(\theta) M_i J_i(\theta)$$

The potential energy of the ith link is given by:

$$V(\theta) = \sum_{i=1}^{n} V_i(\theta) = \sum_{i=1}^{n} m_i g h_i(\theta)$$

The Lagerangian is then:

$$L(\theta,\dot{\theta}) = T(\theta,\dot{\theta}) - V(\theta) = \frac{1}{2}\dot{\theta}^T M(\theta)\dot{\theta} - \sum_{i=1}^{n} m_i g h_i(\theta)$$

The 3-DOF revolute crane as show in Figure 1:

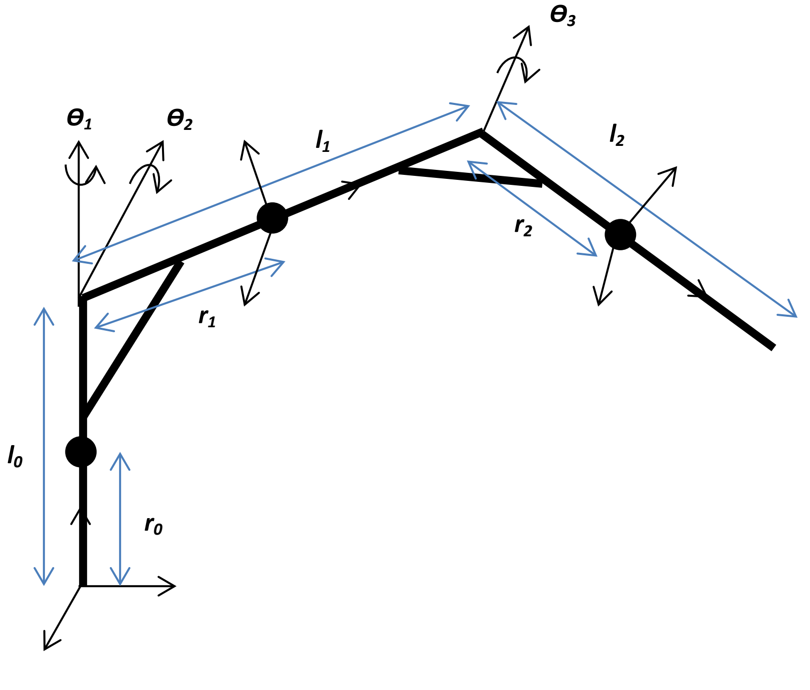

Figure 10 3-DOF revolute crane

The Jacobians:

$$J_1 = \begin{bmatrix} & & \\ & & \\ & & \\ & & \\ & & \\ 1 & & \end{bmatrix}$$

$$J_2 = \begin{bmatrix} -r_1c_2 & & \\ & & \\ & -r_1 & \\ & -1 & \\ -s_2 & & \\ c_2 & & \end{bmatrix}$$

$$J_3 = \begin{bmatrix} -l_2c_2 - r_2c_{23} & & \\ & l_1s_3 & \\ & -r_2 - l_1c_3 & -r_2 \\ & -1 & -1 \\ -s_{23} & & \\ c_{23} & & \end{bmatrix}$$

The blank components are zero, s_i, c_i, s_{ij} and c_{ij} represent $\sin\Theta_i$, $\cos\Theta j$, $\sin(\Theta_{1+}\ \Theta_j)$ and $\cos(\Theta_{1+}\ \Theta_j)$

Same notions apply for the whole text.

The inertia matrix is written:

$$I(\theta) = \begin{bmatrix} I_{11} & I_{12} & I_{13} \\ I_{21} & I_{22} & I_{23} \\ I_{31} & I_{32} & I_{33} \end{bmatrix}$$

The non-zero components are:

$$I_{11} = I_{y2}s_2^2 + I_{y3}s_{23}^2 + I_{z1} + I_{z2}c_2^2 + I_{z3}c_{23}^2 + m_2r_1^2c_2^2 + m_3(l_1c_2 + r_2c_{23})^2$$

$$I_{22} = I_{x2} + I_{x3} + m_3l_1^2 + m_2r_1^2 + m_3r_2^2 + 2m_3l_1r_2c_3$$

$$I_{23} = I_{x3} + m_3r_2^2 + m_3l_1r_2c_3$$

$$I_{32} = I_{x3} + m_3r_2^2 + m_3l_1r_2c_3$$

$$I_{33} = I_{x3} + m_3r_2^2$$

The generalised coordinates for the IC-field:

$$\frac{\partial L}{\partial\dot{\theta}} = \frac{\partial T}{\partial\dot{\theta}} = I(\theta)\dot{\theta}$$

$$\frac{\partial T}{\partial\theta} = \frac{\partial I(\theta)}{\partial\theta}\dot{\theta}_\iota$$

The non-zero components are:

$$C(\theta,\dot{\theta}) = \frac{\partial I(\theta)}{\partial\theta} = \begin{bmatrix} C_{112} * \dot{\theta}_2 + C_{113} * \dot{\theta}_3 & C_{121} * \dot{\theta}_1 & C_{131} * \dot{\theta}_1 \\ C_{211} * \dot{\theta}_1 & C_{223} * \dot{\theta}_3 & C_{232} * \dot{\theta}_2 + C_{233} * \dot{\theta}_3 \\ C_{311} * \dot{\theta}_1 & C_{322} * \dot{\theta}_2 & 0 \end{bmatrix}$$

Where

$$C_{112} = \left(I_{y2} - I_{z2} - m_2r_1^2\right)c_2s_2 + \left(I_{y3} - I_{z3}\right)c_{23}s_{23} - m_3(l_1c_2 + r_2c_{23})(l_1s_2 + r_2s_{23})$$

$$C_{113} = \left(I_{y3} - I_{z3}\right)c_{23}s_{23} - m_3r_2s_{23}(l_1c_2 + r_2c_{23})$$

$$C_{121} = (I_{y2} - I_{z2} - m_2 r_1^2) c_2 s_2 + (I_{y3} - I_{z3}) c_{23} s_{23} - m_3 (l_1 c_2 + r_2 c_{23})(l_1 s_2 + r_2 s_{23})$$
$$C_{131} = (I_{y3} - I_{z3}) c_{23} s_{23} - m_3 r_2 s_{23} (l_1 c_2 + r_2 c_{23})$$
$$C_{223} = -m_3 l_1 r_2 s_3$$
$$C_{232} = -m_3 l_1 r_2 s_3$$
$$C_{233} = -m_3 l_1 r_2 s_3$$
$$C_{311} = (I_{z3} - I_{y3}) c_{23} s_{23} + m_3 r_2 s_{23} (l_1 c_2 + r_2 c_{23})$$
$$C_{322} = m_3 l_1 r_2 s_3$$

$$\frac{\partial V}{\partial \theta} = \begin{bmatrix} 0 & 0 & 0 \\ 0 & -(m_2 g r_1 + m_3 g l_1) c_2 - m_3 r_2 c_{23} & 0 \\ 0 & 0 & -m_3 g r_2 c_{23} \end{bmatrix} \begin{bmatrix} \dot{\theta}_1 \\ \dot{\theta}_2 \\ \dot{\theta}_3 \end{bmatrix}$$

Similar to the previous examples, a BG dynamic model of the crane can be established using IC-field, Figure 11.

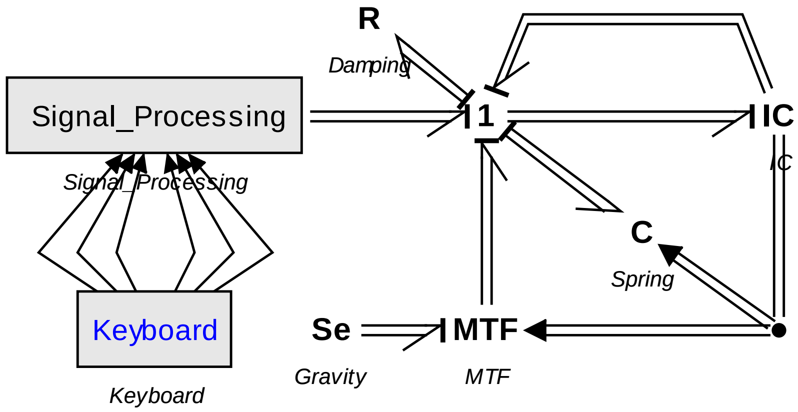

Figure 11. BG model of 3DOF revolute maritime crane

5 WIRE AND PAYLOAD

A lumped model for the wire is represented by a spring-damper along the wire direction, Figure 12. For simplification, the wire is assumed always tensioned.

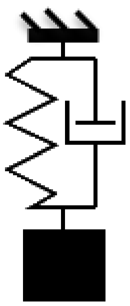

Figure 12. Wire and payload model

The following equations apply for deriving the dynamics of the wire:

Spring-damper force:

$$F = k * \Delta z + c_d \dot{z}$$

The wire stiffness k given by:

$$k = \frac{EA}{l}$$

Where E is the E-modulus of the wire, A is the wire section area and l is the wire length

According to DNV regulations, the metallic cross section area is about 60% of the total area.

$$A = 0.6 * \frac{\pi * d^2}{4}$$

c_d is the wire damping ratio given as a ratio r of the critical damping ratio:

$$c_d = 0.25 * 2\sqrt{mk}$$

6 SIMULATION OF MARITITIME CRANE LIFTING OPERATION

The following equations are presented for deriving the transformer's matrix from the cylinders and crane tip.

The external forces including the gravity force and actuator forces to the crane are represented by transformers (MTF-element). The transforming matrix of the gravity force is given:

$$\mathrm{T}(\theta) = \begin{bmatrix} 0 & 0 & 0 \\ 0 & -(\mathrm{m_2 g r_1} + \mathrm{m_3 g l_1})\mathrm{c_2} - \mathrm{m_3 r_2 c_{23}} & 0 \\ 0 & 0 & -\mathrm{m_3 g r_2 c_{23}} \end{bmatrix}$$

The transforming matrix of the motor and cylinders is given by:

$$\mathrm{T}(\theta) = \begin{bmatrix} 1 & 0 & 0 \\ 0 & \mathrm{a'_1 b'_1} \sin(\theta'_2)/\mathrm{L_1} & 0 \\ 0 & 0 & \mathrm{a'_2 b'_2} \sin(\theta'_3)/\mathrm{L_2} \end{bmatrix}$$

Hence the joint torques are obtained through:

$$\tau(\theta) = \mathrm{T}(\theta)\mathrm{F}$$

Figure 13 shows the illustration in deriving the equations for the two cylinders. The cylinder length as a function of the joint angle is given:

$$\mathrm{L_1} = \sqrt{\mathrm{a'_1}^2 + \mathrm{b'_1}^2 - 2\mathrm{a'_1 b'_1}\cos(\theta'_2)}$$

$$\theta_2 = \arctan\frac{\sin\theta'_2}{\cos\theta'_2} + \arctan\frac{\mathrm{c_{1.1}}}{\mathrm{a_1}} + \arctan\frac{\mathrm{c_{1.2}}}{\mathrm{b_1}} - \frac{\pi}{2}$$

$$\mathrm{L_2} = \sqrt{\mathrm{a'_2}^2 + \mathrm{b'_2}^2 - 2\mathrm{a'_2 b'_2}\cos(\theta'_3)}$$

$$\theta_3 = \arctan\frac{\sin\theta'_3}{\cos\theta'_3} + \arctan\frac{\mathrm{c_{2.1}}}{\mathrm{a_2}} - \arctan\frac{\mathrm{c_{2.2}}}{\mathrm{b_2}} + \pi$$

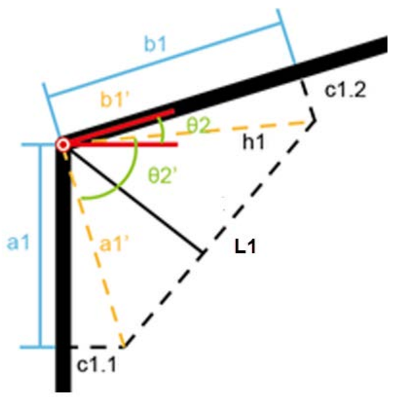

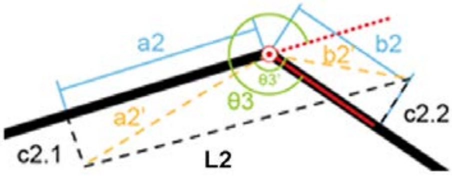

Figure 13. Knuckle boom crane cylinders

To complete the modelling, a transformer is used relating the wire and crane. The Jocobian matrix for computing the crane tip velocity to the joint velocity is given by:

$$J(\theta) = \begin{bmatrix} -l_1s_1c_{23} - l_2s_1c_2 & -l_1c_1s_{23} - l_2c_1s_2 & -l_1c_1s_{23} \\ lc_1c_{23} + l_2c_1c_2 & -l_1s_1s_{23} - l_2s_1s_2 & -l_1s_1s_{23} \\ 0 & l_1c_{23} + l_2c_2 & l_1c_{23} \end{bmatrix}$$

$$v(\theta) = J(\theta)\dot{\theta}$$

A MTF-element is used converting from the joints to the crane tip, i.e. the wire tip.

Based on the above modelling, the integrated model of maritime crane with lifting wire and load can be developed, Figure 14. Using the keyboard as input and the driving forces to the actuators are represented by an MSe-element and transformed to joint torques using MTF-element.

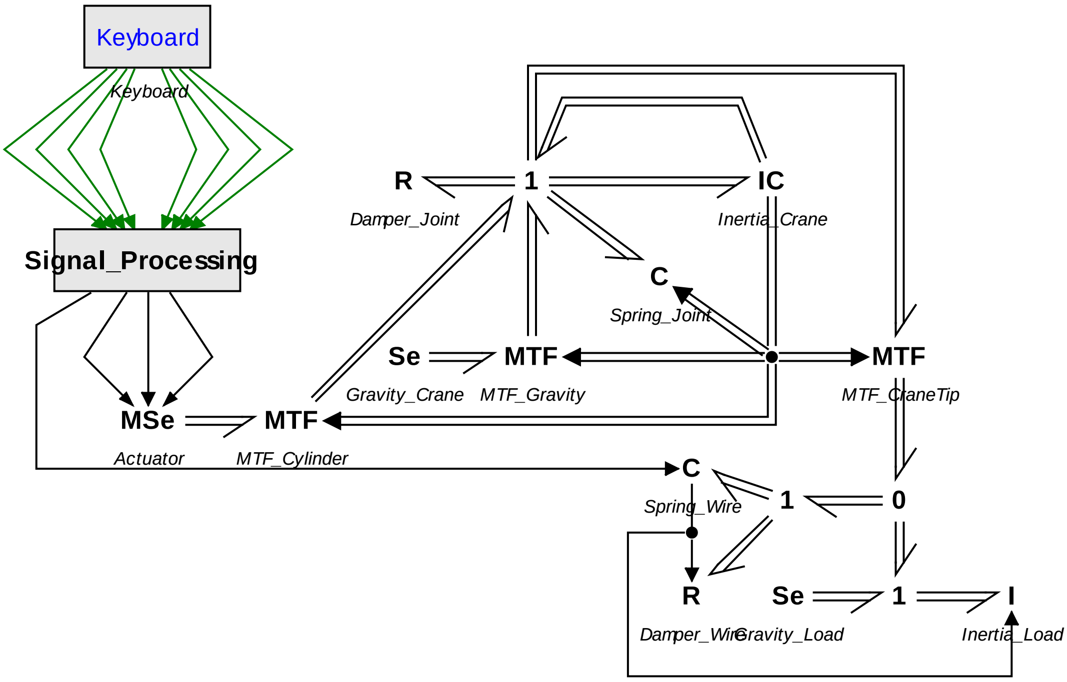

Figure 14. BG model of a 3DOF revolute maritime crane with pendulum load

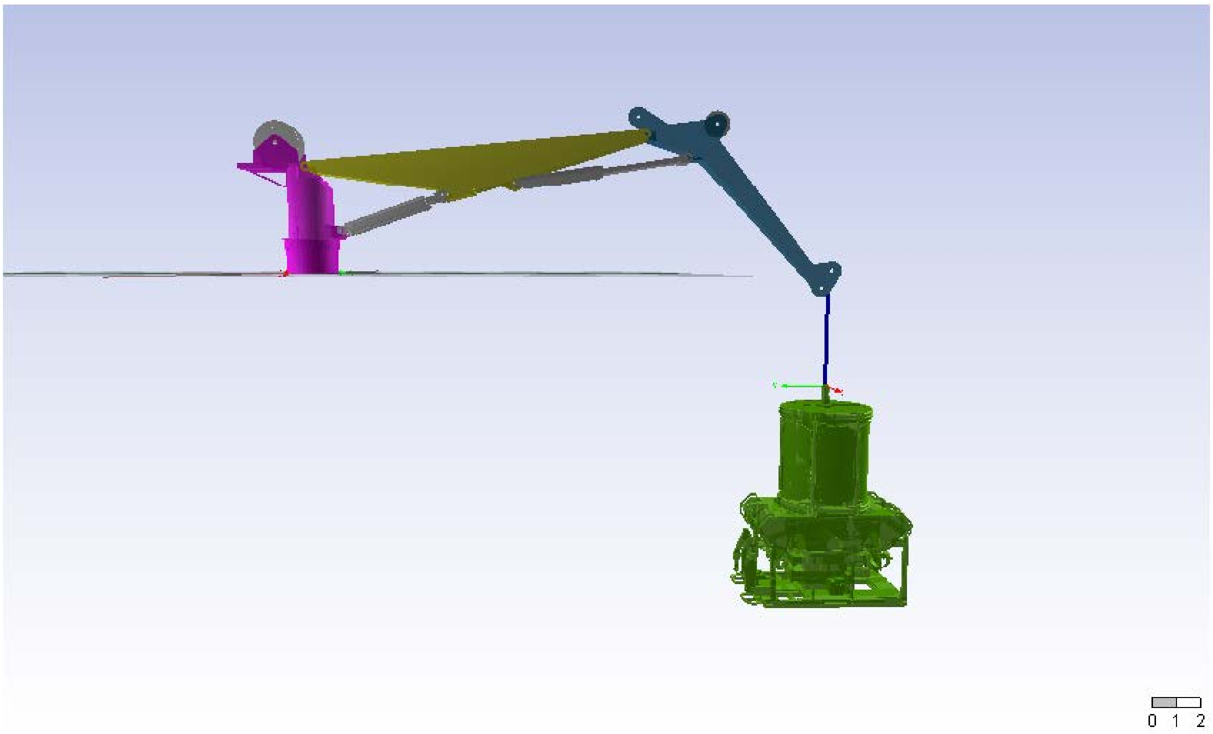

Figure 15. 3D animation scene of maritime crane lifting operation

7 CONCLUSION

The project work in this report presents the modelling process of multi-body dynamics using BG method. Examples from 1D to 2D and 3D multi-body systems are illustrated. As case study, a common type of maritime crane with three degree of freedoms operating in three dimensions is implemented. The BG model of the crane is building block for modelling and simulation of maritime crane operations. Modelling of hydraulic systems and control algorithms including compensation functions can be integrated.

REFERENCE

Karnopp D.C., Margolis D.L. and Rosenberg R.C. *(2012). System Dynamics: Modelling, Simulation, and Control of Mechatronic Systems. John Wiley & Sons, Inc., Hoboken, 5th ed.*

John J. Craig. *(2005). Introduction to Robotics: Mechanics and Control. Prentice Hall. 3rd ed.*

Mark W. Spong and M. Vidyasagar. (2008). Robot Dynamics and Control. Wiley India Pvt. Limited, Student ed.